The Journal of Experimental Biology 202, 1229–1241 (1999)
Printed in Great Britain © The Company of Biologists Limited 1999
JEB2082

THE ELECTRIC ORGAN DISCHARGE OF PULSE GYMNOTIFORMS: THE TRANSFORMATION OF A SIMPLE IMPULSE INTO A COMPLEX SPATIO-TEMPORAL ELECTROMOTOR PATTERN

ANGEL ARIEL CAPUTI*

Division Neuroanatomia Comparada, Instituto de Investigaciones Biológicas Clemente Estable, Avenue Italia 3318, Montevideo, Uruguay

*e-mail: angel@iibce.edu.uy

Accepted 25 January; published on WWW 21 April 1999

Summary

An understanding of how the nervous system processes an impulse-like input to yield a stereotyped, species-specific electromotor output is relevant for electric fish physiology, but also for understanding the general mechanisms of coordination of effector patterns. In pulse gymnotids, the electromotor system is repetitively activated by impulse-like signals generated by a pacemaker nucleus in the medulla. This nucleus activates a set of relay cells whose axons descend along the spinal cord and project to electromotor neurones which, in turn, project to electrocytes. Relay neurones, electromotor neurones and electrocytes may be considered as layers of a network arranged with a lattice hierarchy. This network is able to coordinate a spatio-temporal pattern of postsynaptic and action currents generated by the electrocyte membranes. Electrocytes may be innervated at their rostral face, at their caudal face or at both faces, depending on the site of the organ and the species. Thus, the species-specific electric organ discharge patterns depend on the electric organ innervation pattern and on the coordinated activation of the electrocyte faces. The activity of equally oriented faces is synchronised by a synergistic combination of delay lines. The activation of oppositely oriented faces is coordinated in a precise sequence resulting from the orderly recruitment of subsets of electromotor neurones according to the 'size principle' and to their position along the spinal cord. The body of the animal filters the electric organ output electrically, and the whole fish is transformed into a distributed electric source.

Key words: electric organ discharge, innervation pattern, electromotor system, motor control, electric fish, gymnotiform.

Introduction

Weakly electric fish produce electric fields that are not strong enough for prey capture or defence but convey signals for communication and exploration of the nearby environment (Lissmann, 1951). Two main orders of weakly electric fish have evolved in parallel: the Mormyriformes in Africa and the Gymnotiformes in America (see Bullock and Heiligenberg, 1986; Finger et al., 1986; Kramer 1990; Moller, 1995). Weakly electric fish are also classified as 'wave' species and 'pulse' species. In 'wave' fish, the interval between consecutive electric organ discharges (EODs) is so short that single events fuse, forming a continuous wave. Conversely, in 'pulse' fish, the interval is much longer than the EOD. Both wave and pulse species are represented in both the African and American groups (Bass, 1986; Hopkins, 1995).

In pulse gymnotids, the electromotor system is repetitively activated by a simple, impulse-like input generated by a set of electrotonically coupled pacemaker neurones located in the medulla. This signal triggers the coordinated activation of hundreds of effector units in the electric organ (EO) (Macadar, 1993). Because of EO activation, the whole fish body becomes an electric source. Currents derived from loading this source with the surrounding impedance are sensed by the same fish (electrolocation signals; Lissmann, 1951; Bastian, 1986; Bell, 1989) and by conspecifics (electrocommunication signals; Black-Cleworth, 1970; Hopkins, 1981; Kramer, 1990; Moller, 1995).

This article is concerned with the mechanisms responsible for electrogenesis in pulse gymnotids. It is focused on the best-studied species (*Gymnotus carapo*). Reference is also made to comparative studies in less-known species, *Brachyhypopomus pinnicaudatus* and *Rhamphichthys rostratus*, to illustrate common anatomo-functional designs and species-specific variations.

The electric organ discharge

The simplicity of the input (the synchronised discharge of the pacemaker cells) contrasts sharply with the complexity of the output of the electromotor system. This output is in fact difficult to characterise. One common method is to record in

water the temporal course of the head-to-tail EOD-associated field (Coates et al., 1954). These waveforms can be broken down into segments that are referred to as EOD wave components (N, P and V_1–V_5) (Fig. 1). The number, polarity and sequence of wave components are typical of each species (Bullock et al., 1979; P and N for *Brachyhypopomus pinnicaudatus*, Hopkins et al., 1990; V_1–V_4 for *Gymnotus carapo*, Trujillo-Cenóz et al., 1984; and V_1–V_5 for *Rhamphichthys rostratus*, Caputi et al., 1994).

However, the head-to-tail approach oversimplifies the description of the EOD-associated field potential. In each of these species, field potentials recorded in the water along the fish body show site-specific, multiphasic waveforms that reveal the true spatio-temporal complexity of the EOD (Bennett, 1971; Watson and Bastian, 1979; Caputi et al., 1989, 1994, 1998). Fig. 2 shows an example from *G. carapo*. On the basis of these data, it is possible to calculate the distribution of charge that may cause the external EOD-associated fields (Hoshimiya et al., 1980; Rasnow et al., 1993; Rasnow, 1996; Rasnow and Bower, 1996). However, the solution of the so-called 'inverse problem' (i.e. the calculation of the source from external measurements) is not unique (Helmholtz, 1853; Lopez da Silva and van Rotterdam, 1982). Thus, recordings in water are not adequate to describe the electric source equivalent to the fish body during the EOD.

The electromotor system gives the fish the ability to emit external currents; such an ability is the necessary consequence of the system activity. The EOD-associated electric field is a contingent consequence of loading the system by a particular distribution of impedance in the surrounding medium. Thus, for maximal generality, the output of the electromotor system

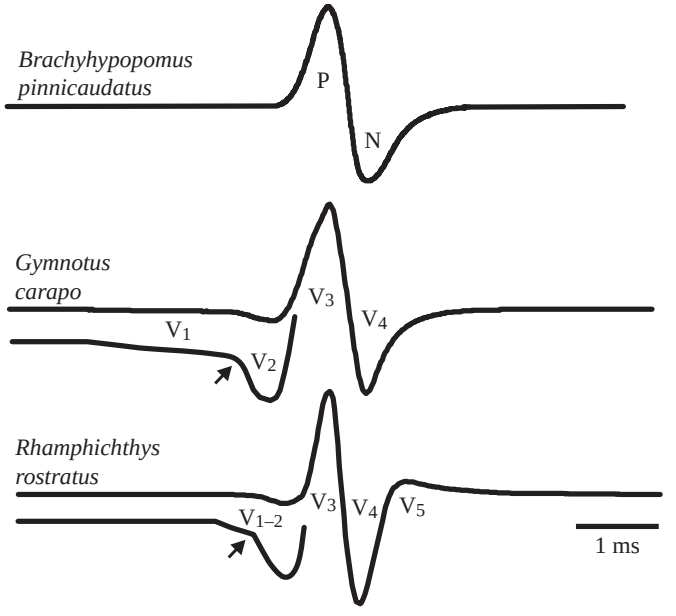

Fig. 1. Head-to-tail electric organ discharge (EOD)-associated electric fields recorded in water. Wave components (N, P and V_1–V_5) observed in three species of pulse gymnotiforms: (A) *Brachyhypopomus pinnicaudatus*; (B) *Gymnotus carapo*; and (C) *Rhamphichthys rostratus*. Arrows indicate the transition between V_1 and V_2.

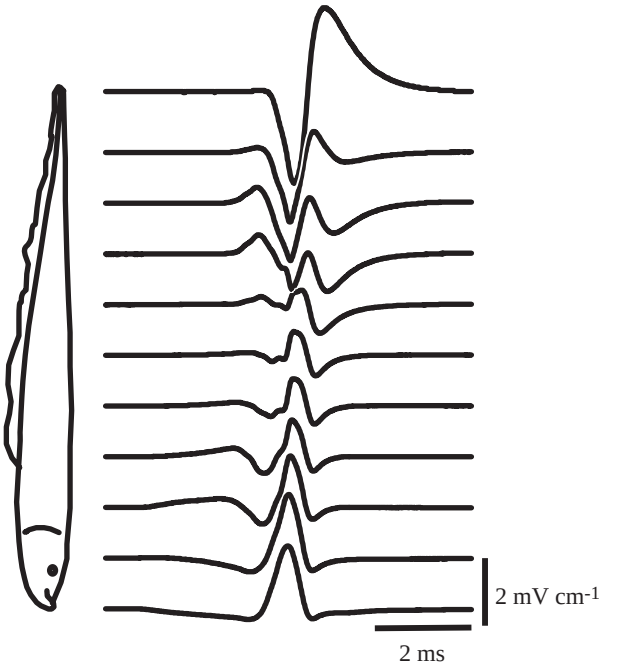

Fig. 2. Electric organ discharge (EOD)-associated electric fields recorded in water. Temporal profiles were recorded perpendicular to the fish axis at 11 equally spaced sites along a line parallel to the body of *Gymnotus carapo*.

should be defined as the electrically equivalent source and should be described by the parameters of that source.

To assess the equivalent electric source, one must determine the parameters that permit the solution of the so-called 'forward problem', i.e. the calculation of surrounding fields and current densities (Fessard, 1958; Lopez da Silva and van Rotterdam, 1982). These parameters describe the equivalent source and the loading impedance. To assess the source parameters, Cox and Coates (1938) introduced voltage recordings obtained with the fish's body electrically isolated in air (see also Coates et al., 1937, 1940; Harder et al., 1964; Bell et al., 1976). This technique is referred to subsequently as 'the air-gap method' (Caputi et al., 1989). This method allows one to describe the equivalent electric source unambiguously by measuring the Thevenin parameters (electromotive force, EMF, and internal series resistance, R_i; Donaldson, 1958).

In *G. carapo*, when the head-to-tail EOD is recorded in air-gap conditions and the electrodes are connected by load resistors, the EOD amplitude varies with load resistance but the waveform remains constant. At any given time, the drop in voltage between the ends of the load resistor is a linear, but decreasing, function of the current flowing through the circuit (Fig. 3C). The ordinate intercept of this function corresponds to the equivalent electromotive force (EMF), and the slope of the line corresponds to the internal series resistance (R_i) of the equivalent generator. The magnitude and waveform of the EMFs are species-specific and independent of the fish's length. Conversely, the R_i of the whole fish body is an inverse function of the fish's length (Fig. 3).

The distribution of the EMF and R_i along the fish can be estimated by making air-gap recordings encompassing different portions of the fish body (Caputi et al., 1989). The passive longitudinal resistance was found to be similar to the R_i of the same portions of the fish. Thus, it was concluded that the resistance of the surrounding tissues, connected in parallel to the EO, 'clamps' the R_i of the equivalent source (Caputi and Budelli, 1995). However, an important exception to this general rule is the occurrence of load-dependent variations in the last negative wave component, as observed in some specimens of *G. carapo* and also in sexually dimorphic *B. pinnicaudatus* (see below).

Recordings made in water suggested that the fish body is a distributed bioelectric source. To test this hypothesis, multiple simultaneous air-gap recordings were made between pairs of electrodes encompassing consecutive portions of the body all along the fish (Caputi et al., 1993). We found that wave components can be characterised by their longitudinal domains, their timing and their relative regional amplitudes. They are also different in their generation mechanisms.

The multiple air-gap technique permitted us to identify four features common to pulse gymnotids (Fig. 4): (1) different wave components arise at different portions of the EO; (2) the EMF generated per unit length of the fish increases exponentially in the rostro-caudal direction, but at a different rate for each wave component; (3) there is a very fast rostro-caudal order of activation of the EO; and (4) the EMF pattern generated in the abdominal portion is the most complex and species-specific (Caputi et al., 1993, 1994, 1998).

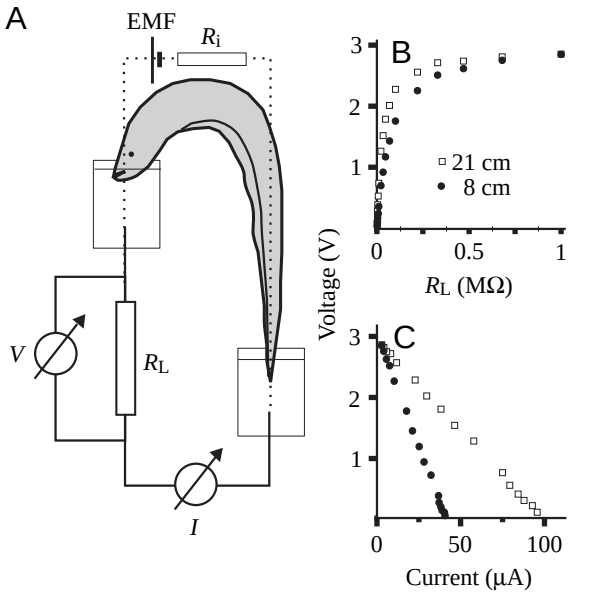

Fig. 3. Equivalent electric source parameters. (A) Schematic diagram of the air-gap recording system. *V* is the voltage drop across the load resistance R_L, and *I* is the current through the circuit. (B) Voltage across R_L as a function of R_L. (C) Voltage across R_L as a function of the current (both measured at the peak of phase V_3 of the electric organ discharge in two fish 8 and 20 cm in length). Note that, in spite of the difference in length, the ordinate intersection (the electromotive force, EMF) in C is approximately the same while the slope of the line (R_i) decreases with animal length. V=EMF–R_iI.

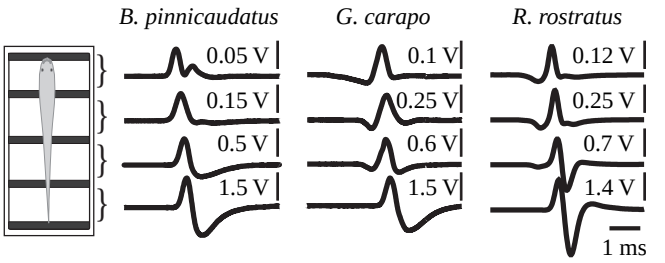

Fig. 4. Electromotor patterns in three species of pulse gymnotids. The fish lies through alternated conductive and non-conductive compartments. Each conductive compartment was connected to a high-input-impedance unity-gain non-inverting buffer amplifier with their outputs connected to differential amplifiers. In such conditions, the external currents are negligible, and the recorded voltages are equivalent to the electromotive force (EMF). This procedure avoids load-sharing and permits one to obtain the output of each portion independently of the others. For the same reason, it is impossible to measure the internal resistance using this procedure. (A) *Brachyhypopomus pinnicaudatus*; (B) *Gymnotus carapo*; (C) *Rhamphichthys rostratus.*

Knowledge of the electromotive force pattern is necessary but is not sufficient to describe the fish's body as an electric source (Fessard, 1958). Geometrical parameters and fish tissue resistance must also be known to calculate the external EOD field. R_i is partially determined by the length and shape of the fish body. Since specimens of different length are geometrically similar, the total internal resistance is an inverse function of fish length. Modelling work taking into account fish geometry and the specific resistance of the tissues accurately predicted the EOD-associated electric field and the transepidermal currents recorded experimentally (Caputi and Budelli, 1995; Caputi et al., 1998).

During the breeding season, males and females of *B. pinnicaudatus* show anatomical and EOD waveform differences (Hopkins et al., 1990). Both the P–N transition and the N-wave duration are prolonged in males. Interestingly, these waveform differences are only observed when recorded in water, while the spatio-temporal patterns of EMFs recorded using the multiple air-gap technique show no significant differences between sexes (Fig. 5A). Two independent processes probably account for this differences. First, the internal resistance distribution follows the shape of the fish body and, therefore, the resistance of the tissues surrounding the EO is lower in the thick tail of males than in the thin tail of females. Second, the N/P ratio increases with load in both males and females (Fig. 5B). The concomitant decrease in duration of the N-wave indicates an additional change in the EMF as a function of the load resistance.

This phenomenon, also present in some *G. carapo*, may be similar to that observed by Bell et al. (1976) in mormyrids in which the head-negative wave EMF is load-dependent. The late waves generally derive from action potential propagation from the innervated face of the electrocyte to the non-

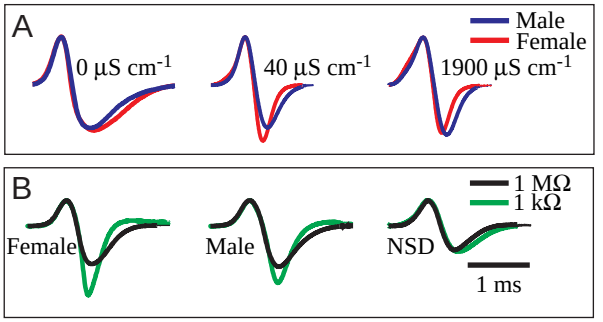

Fig. 5. Head-to-tail electric organ discharge (EOD) waveform variations caused by external load in *Brachyhypopomus pinnicaudatus*. Waveforms normalised with regard to the maximum are superimposed to compare the different load effects in male and females. (A) Male (blue) and female (red) waveforms were compared in three experimental conditions: (left) air-gap recordings with infinite load resistance; (middle) recordings in water of 40 µS cm^{-1}; (right) recordings in water of 1900 µS cm^{-1}. (B) Load effect on the N-wave of the electric organ discharge recorded in air-gap conditions. Superimposed traces show normalised waveforms obtained in the same fish using two load resistors (1 kΩ, green; 1 MΩ, black). Note that lowering the load resistance provokes a relative increase in amplitude but a decrease in duration of the N-wave in sexually dimorphic males and females. The amplitude of the N-wave remains unchanged in undifferentiated fish (NSD).

innervated face. Thus, low-resistance pathways, external to the EO, facilitate action potential propagation along the electrocyte membrane. Interestingly, the waveform of *B. pinnicaudatus*, which shows no sexual differentiation, was much less affected by load, suggesting that the change in the N/P ratio is a hormone-dependent process (Fig. 5B).

Finally, since fish are poikilotherms living in a medium of high specific heat, electrogeneration is affected by external temperature. The change observed in the amplitude of the late negative wave in *G. carapo* (V_4) and *B. pinnicaudatus* (N) (Ardanaz, 1998; Caputi et al., 1998) is a particularly noteworthy effect. This effect occurs in nature in *B. pinnicaudatus* (Silva et al., 1996). Since the effect is less marked in males than in females, it may play a role in sexual communication and reproduction.

The electric organ and its innervation pattern

In pulse gymnotids, the EO extends from the anal papilla to the tip of the tail. The EOs are composed of several tubes containing series of cells called electrocytes (formerly electroplaques). The discharge results from the sum of postsynaptic currents and action currents generated in hundreds of electrocytes whose active membranes are similarly oriented and simultaneously activated.

Long before these currents were measured in individual electrocytes, Paccini established that ‘the innervated faces of the electroplaques become negative during the discharge whatever the orientation of the organ’ (cited by Keynes et al., 1961). This rule implies that the innervation pattern of the EO is a major determinant of the EOD waveform. Thus, knowledge of this pattern is crucial for understanding mechanisms of waveform generation.

Schaffer (1917) showed that the EO of *G. carapo* is composed of four longitudinal tubes containing rows of electrocytes on each side of the body. However, he did not describe the innervation pattern of the EO. This pattern was still not well understood when Bennett and Grundfest (1959) proposed a hypothesis for EOD waveform generation based on simultaneous intracellular and extracellular recordings of single electrocytes. They reported the existence of two different sets of electrocytes: rostrally innervated electrocytes in the more dorsal tube (tube 1) and caudally innervated electrocytes in the other three tubes (tubes 2, 3 and 4). To explain the triphasic temporal pattern of the EOD, they postulated that activation of rostrally innervated electrocytes generated the first head-negative deflection, that activation of the caudally innervated electrocytes generated the head-positive deflection and that the action currents generated at the innervated caudal face excited the opposite electrocyte face, generating the late negative deflection.

Szabo (1960) showed that the electrocytes of tube 1 are innervated not only on their rostral face but also on their caudal face in the central region of the body of *G. carapo*. In a subsequent study, Szabo (1961) observed that the length of the tubes was not the same. Tube 1 (containing doubly innervated electrocytes) and tube 2 (containing caudally innervated electrocytes) extended within the abdominal wall to the anal papilla, while the other tubes did not. In contrast, Couceiro and De Almeida (1961) reported that electrocytes in the caudal portion of the EO are innervated exclusively on their caudal face.

Trujillo-Cenóz et al. (1984) identified an early wave component (V_1) in *G. carapo* and showed that it was generated in the abdominal portion of tube 1 where the doubly innervated electrocytes occur. While fibres arising from spinal roots I–VII innervate the rostral face of doubly innervated electrocytes, fibres arising from spinal roots VIII–XIII innervate the caudal face of all abdominal electrocytes. This last group of fibres projects to the abdominal region as a recurrent nerve (the anterior electromotor nerve, AEN). When the spinal cord was transected at the level of spinal root VIII, only the early, head-negative deflection (V_1) remained unchanged. Moreover, when the abdominal portion of the EO was damaged, this wave component disappeared. Thus, it was concluded that V_1 is generated by activation of the rostral face of doubly innervated electrocytes lying in the abdominal portion of tube 1.

In a subsequent report, Trujillo-Cenóz and Echagüe (1989) described three different zones in the EO according to their innervation pattern (see Fig. 9). They showed that tube 1 has doubly innervated electrocytes in its abdominal and central portions, but not in its caudal portion. The other tubes contain only caudally, singly innervated electrocytes. In addition, they described a pair of posterior electromotor nerves (PENs) containing the fibres innervating the caudal region of the EO. Thus, the paradoxical results of Szabó (1961) and Couceiro

and De Almeida (1961) concerning the innervation of tube 1 were explained by the heterogeneous pattern of innervation of the EO.

Lorenzo et al. (1988) confirmed the spatial origin of V_1 and demonstrated that this wave component of the EOD results from postsynaptic potentials elicited in the rostral face of electrocytes by terminal branches of segmental nerves. They also showed that the other component generated in this region (V_3) originates from action potentials evoked by nerve excitation of the caudal face of all abdominal electrocytes.

Macadar et al. (1989) ratified the findings of Lorenzo et al. (1988) and were able to reproduce the regional EOD waveform by activating a single electrocyte using paired stimulation of the AEN and the segmental nerve (Fig. 6A). Their experiments also confirmed the data of Bennett and Grundfest (1959) for the central portion of the fish body (Fig. 6B). In addition, they showed that electrical stimulation of the PEN causes the action potentials arising on the caudal face of singly innervated electrocytes of the tail region. These action potentials, in turn, evoked spikes on the rostral electrocyte face (Fig. 6C). The final negative wave (V_4 in *G. carapo* and *R. rostratus*, and N in *B. pinnicaudatus*) is due to the summation of these rostral-face spikes. Consistently, partial curarization reduced V_3 and abolished V_4 (Caputi et al., 1989, 1994, 1998).

Comparative studies in *B. pinnicaudatus* and *R. rostratus* confirmed that the polarity and spatial origin of each wave component are mainly determined by the EO innervation pattern (Fig. 7). *B. pinnicaudatus* exhibits a single type of singly innervated electrocyte. As in *G. carapo*, two pairs of tubes extend from the tip of the tail to the anal papilla, while the other tubes do not extend beyond the rostral edge of the anal fin, but all electrocytes are caudally innervated (Trujillo-Cenóz et al., 1984). This simple innervation plan is consistent with the observed biphasic head-to-tail EOD waveform and with the spatiotemporal pattern of the EMF (Caputi et al., 1998). In contrast, *R. rostratus* shows three types of electrocyte with dissimilar innervation pattern: caudally innervated, rostrally innervated and marginal-caudally innervated. This variety supports a more complex pattern that exhibits five wave components. In the subopercular region, the EO of *R. rostratus* consists of a pair of tubes containing only caudally innervated electrocytes. In the abdominal region, the EO consists of three pairs of tubes. Each pair contains one of the described electrocyte types. In the central region, most tubes contain doubly innervated electrocytes, and in the caudal 25% exclusively caudally innervated electrocytes occur.

Air-gap experiments indicated that V_1 results from the activity of the rostral face of rostrally innervated electrocytes, V_2 results from the activities of the rostral face of marginal-caudally innervated electrocytes and V_3 results from the activities of the caudal face of most electrocytes. Curarization experiments showed that V_4 and V_5 are not directly elicited by neural activity (Caputi et al., 1994).

It is important to note that two of the three known families of pulse gymnotids exhibit doubly innervated electrocytes. In the case of *Rhamphichthys*, doubly innervated electrocytes

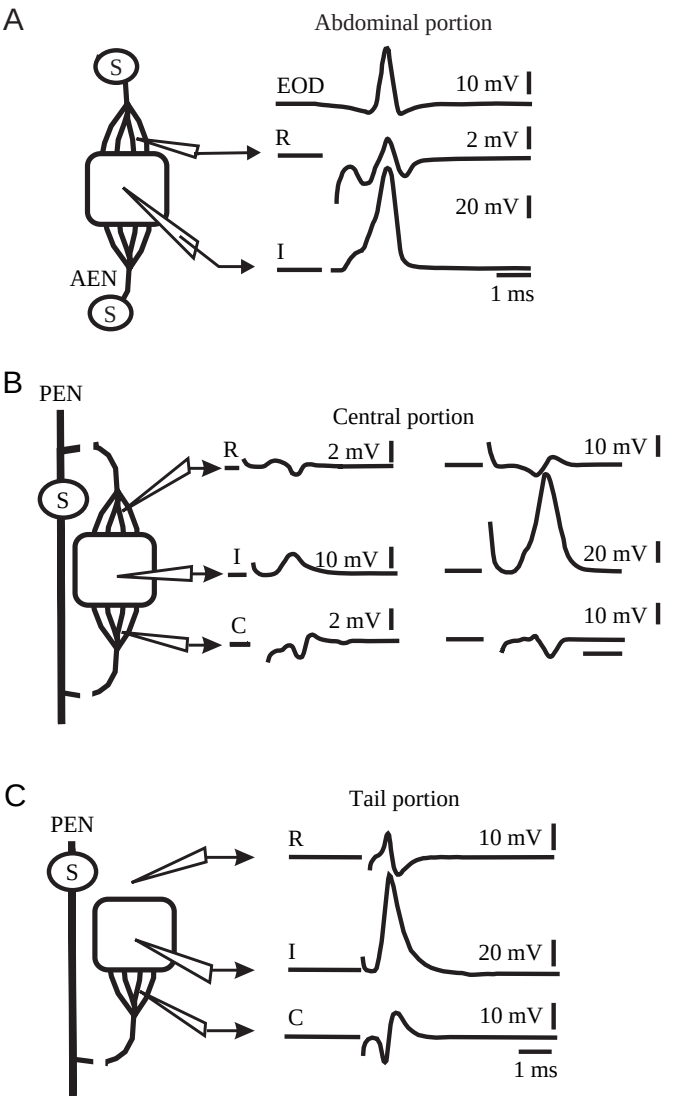

Fig. 6. Simultaneous extracellular and intracellular recordings of electrocyte activity evoked by the stimulation of their afferent nerves. (A) Recordings made in the abdominal portion of the fish. Stimuli (S) to the anterior electromotor (AEN) and segmental nerves were timed to obtain an intracellular response similar to that observed during spontaneous activation of an electrocyte (I). In this condition, the extracellular triphasic wave (R) recorded at the rostral face of the electrocyte resembles the electric organ discharge (EOD) waveform in the intact fish. (B) Recordings made in the central portion of the fish. Left, submaximal stimulation of the posterior electromotor nerve (PEN) generated a postsynaptic potential in the electrocyte (I); extracellular recordings show that under these stimulation conditions, the caudal face of the electrocyte was stimulated earlier than the rostral face (compare C and R). Right, more intense stimulation of the PEN elicited an action potential in the electrocyte (I). This response is generated in the rostral face (R), where an initial sink of current is observed. (C) Recordings made in the tail portion of the fish. Stimulation of the PEN elicited an action potential in the electrocyte (I). This response is generated in the caudal face (R) where an initial sink of current is observed. The action potential appears to be propagated to the caudal face (C), where the recordings are mirror images of those taken at the opposite face (modified from Macadar et al., 1989).

show three distinctive features: (a) the nerve fibres arriving at the rostral side form a regular palisade all over the electrocyte margin; (b) synaptic junctions occur in the marginal membrane; and (c) the caudal faces bear large ridges receiving most of the caudal innervation (Fig. 8).

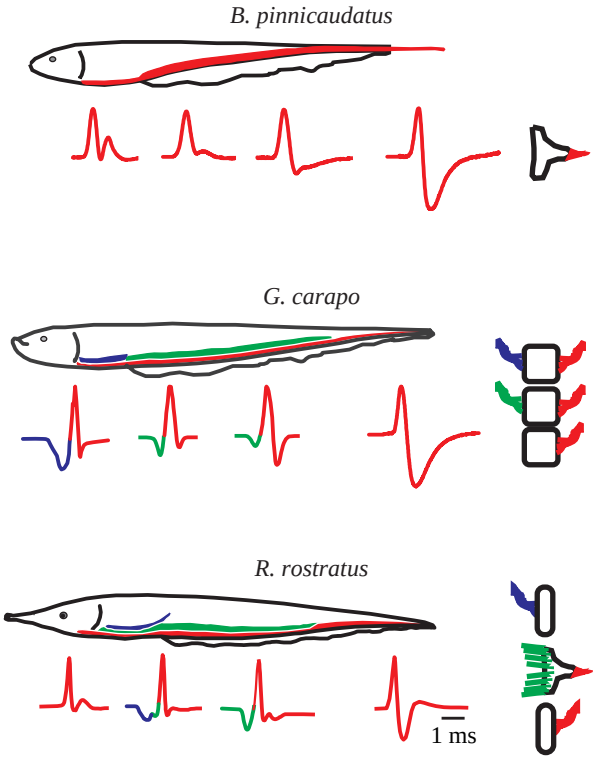

Fig. 7. This semi-schematic drawing correlates different electric organ (EO) portions with samples of the regional electric organ discharges (EODs) recorded in air-gap conditions in three species. It also illustrates the distribution of the different electrocyte types along the EO. *Brachyhypopomus pinnicaudatus* bears only caudally innervated electrocytes and the EOD shows a simple biphasic waveform. Note, however, the different ratio between the head-positive wave component (due to the neurally evoked action potential) and the head-negative wave component (due to action potential propagation) at different sites on the fish. *Gymnotus carapo* bears three types of electrocyte according to their innervation pattern and membrane properties. Doubly innervated abdominal electrocytes with no action potential responses in the rostral face (blue), doubly innervated intermediate electrocytes with action potential responses in the rostral face (green), and caudally innervated electrocytes (red). Note the correlation between the location of different types of electrocytes and the wave components present in the regional EODs. V_1 occurs at the abdominal level (blue), V_2 at the intermediate portion (green), V_3 is present all along the fish body, and the tail exhibits a simple biphasic waveform (V_3–V_4, red). *Rhamphichthys rostratus* bears three types of electrocyte according to their innervation pattern. Rostrally innervated (blue), marginal-caudally innervated (green) and caudally innervated (red) electrocytes. Note the correlation between the location of different types of electrocyte and the wave components present in the regional EODs. V_1 occurs at the abdominal level (blue), V_2 at the abdominal and the intermediate portions (green), V_3 (red) is present all along the fish body, and the tail exhibits a triphasic waveform (V_3–V_4–V_5, red). The late V_5, as well as the ripples observed in the more rostral recordings of *B. pinnicaudatus* and *R. rostratus*, may correspond to oscillatory responses of the electrocyte caused by field effects on the electrocyte membrane or on the fine nerve terminals.

In addition to the innervation pattern, other factors are important in determining the EOD waveform. (1) The extended EO of pulse gymnotids exhibits a non-uniform density of electrocytes whose sizes and separations diminish exponentially from head to tail. Consistently, the amplitude of the local EOD shows a similar exponential increment along the EO, indicating that the amplitude of the local EOD is proportional to the number of generating units. (2) The ratio between the amplitude of the non-neurally triggered, late wave components and the amplitude of their preceding waves is not constant along the fish body in all three genera. Since these wave components are due to the propagation of the neurally elicited action potentials from the innervated to the non-innervated face of the electrocytes, a mechanism that is still not well understood and that determines the site-dependent efficiency of action potential propagation along the electrocyte membrane must be present. (3) In *Brachyhypopomus*, the N-wave (and thus action potential propagation) is under endocrine and thermal control (Hagedorn and Carr, 1985; Hopkins et al., 1990; Franchina, 1993; Silva et al., 1996; Caputi et al., 1998). Thus, it is probable that plastic membrane properties may play a major role in determining the shape of this wave component.

Similar phenomena have been observed in wave gymnotids (Mills and Zakon, 1987; Zakon et al., 1991a,b; Ferrari and Zakon, 1993; Zakon, 1993) and pulse mormyrids (Toerring and Serrier, 1978; Bass and Hopkins, 1983; Landsman and Moller, 1988).

Finally, *B. pinnicaudatus* and *R. rostratus* show a second positive wave component in the abdominal region, where only caudally innervated electrocytes occur. Since this second wave component is suppressed by partial curarization (A. A. Caputi,

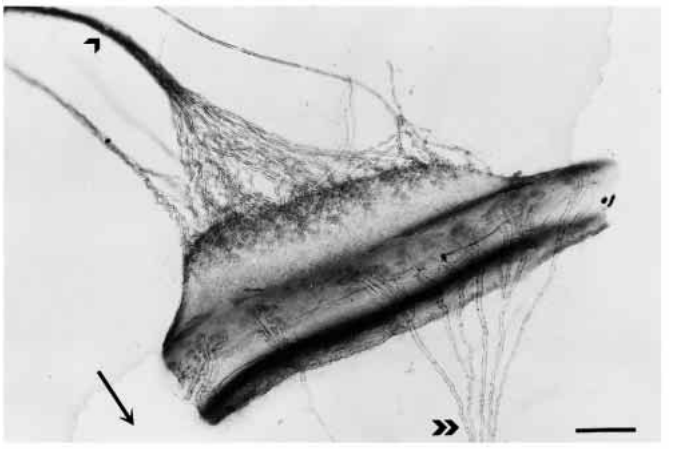

Fig. 8. Photomontage covering two focal planes of an osmium-stained doubly innervated electrocyte of *Rhamphichthys rostratus*. The arrowheads indicate the axon bundles terminating in the caudal ridge (single arrowheads) and in the electrocyte margin (double arrowheads). The arrow on the left points rostrally, indicating the position of the electrocyte. Scale bar, 350 µm. (Modified from Caputi et al., 1994.)

unpublished observations), it probably results from field effects either on other electrocyte membranes or on the terminal branches of the AEN (Albe-Fessard and Buser, 1950; Bennett and Grundfest, 1959).

The neural network

Each wave component arises from the activation of a subset of similarly innervated electrocytes, located at specific regions of the EO and firing synchronously at a given phase after the pacemaker nucleus. Thus, to organise the stereotyped pattern of activation of the EO, the nervous system must determine the timing of activation of the electrocytes. Electrocytes belonging to the same subset must be synchronously activated, and different subsets have to be recruited in the temporally correct order.

The performance of these tasks depends on interactions among three types of excitable cells: the relay neurones (RN), the electromotor neurones (EMNs) and the electrocytes. RNs project onto EMNs, which in turn project onto electrocytes. At both projection levels, there is convergence and divergence. Thus, each subset of excitable cells may be considered as a layer of a network arranged with a lattice hierarchy (Camhi, 1984).

Below the pacemaker, at the ventral surface of the medulla, a group of 70–90 RNs receive the synchronous input from the pacemaker cells (Trujillo-Cenóz et al., 1990; Lorenzo et al., 1993). The RN axons form the bulbo-spinal electromotor tract at the dorso-lateral column of the spinal cord. While some of the RN axons extend from the medulla to the caudal segments of the cord, others end at intermediate or relatively rostral levels (Ellis and Szabo, 1980). The diameters and conduction velocities of the axons appear to be correlated with their lengths (Mezler et al., 1974; Lorenzo et al., 1990). Slowly conducting fibres make up 40 % of the total in the rostral segments, while they are absent in the caudal three-quarters of the spinal cord. Conversely, a large proportion (40 %) of fast-conducting fibres is present in the caudal portion (Lorenzo et al., 1990).

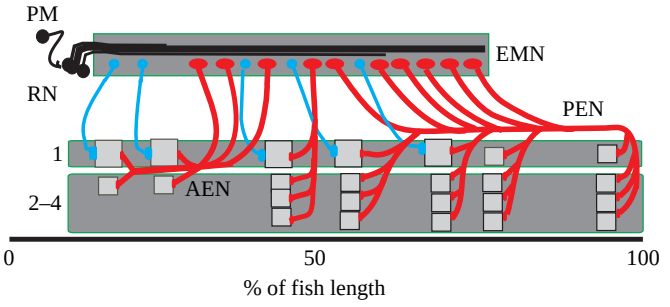

Fig. 9. Schematic drawing of the neural network subserving coordination of electric organ (EO) activation. The network consists of three logical layers. The relay neurones (RNs) project onto the electromotor neurones (EMNs), which in turn project onto the electrocytes. The electrocytes are contained in connective tubes. Tube 1 contains doubly innervated electrocytes in its rostral three-quarters, while the other tubes (tubes 2–4) contain exclusively caudally innervated electrocytes. There are convergent and divergent connections in both layers and a species-specific pattern of innervation of the EO. AEN, anterior electromotor nerve; PEN, posterior electromotor nerve; PM, pacemaker cells.

Bennett et al. (1964, 1967) showed that the RN axons and the EMN somata were coupled by electric synapses. In *G. carapo*, contacts between RN terminals and the EMNs exhibit the morphological specialisation characteristic of mixed synapses (Bennett et al., 1978; Baillet Derbin, 1988; Trujillo-Cenóz et al., 1986). Two main classes of synaptic connection (both of the mixed type) can be observed: (a) 'boutons' corresponding to terminations of myelinated or unmyelinated fibres and (b) synapses '*en passant*' usually originating from the nodes of Ranvier (Trujillo-Cenóz et al., 1986). EMN dendrites extend in the rostro-caudal direction, running close to neighbouring EMN somata. It is not unusual for a single RN 'bouton' to make contact with a dendrite and a soma pertaining to different EMNs.

Functional data confirm convergence (contacts from multiple RN axons on a single EMN) as well as divergence (contacts of a single axon with various and relatively distant EMNs). In some cases, intracellular stimulation of a single RN activated a large population of electrocytes distributed along a large portion of the EO. In others, no EO responses were obtained, suggesting that some EMNs only fire if they are activated by more than one RN axon (Lorenzo et al., 1993).

EMN location along the spinal cord is linearly related to their projection site along the EO. However, horseradish peroxidase injections not exceeding 5 % of the EO labelled EMN arrays occupying up to 20 % of spinal cord length (Caputi and Trujillo-Cenóz, 1994). This dispersion is in agreement with the reduction, but not abolition, of the regional EODs when a relatively small portion of the spinal cord was surgically removed (Caputi et al., 1993). This indicates that there is convergence of distant EMNs onto the same site of the EO and divergence of adjacent EMNs to distant sites of the EO.

This network (Fig. 9) is able to synchronise the activity of homologous electrocyte faces by a synergetic combination of delay lines. On the basis of the study of Lorenzo et al. (1990), Aguilera and Caputi (1995) modelled the activity of the bulbo-spinal tract. The results from this model are in agreement with the field potential recordings of the bulbo-spinal tract at different sites along the spinal cord (Caputi and Aguilera, 1996). At the rostral end of the spinal cord, the population of RNs is heterogeneous in diameter and conduction velocity; thus, the composite action potential would peak at an intermediate delay between fast and slow fibres. At the caudal end of the spinal cord, the population of RNs is composed almost exclusively of large and fast fibres; thus, the composite action potential would peak at the delay set by the fast fibres. Consequently, the delay from the pacemaker discharge to the peak of the composite action potential will be an increasing (but not linear) function of the distance from the pacemaker to the site of recording (Fig. 10). These data are in agreement with the mechanism of synchrony described by Lorenzo et al.

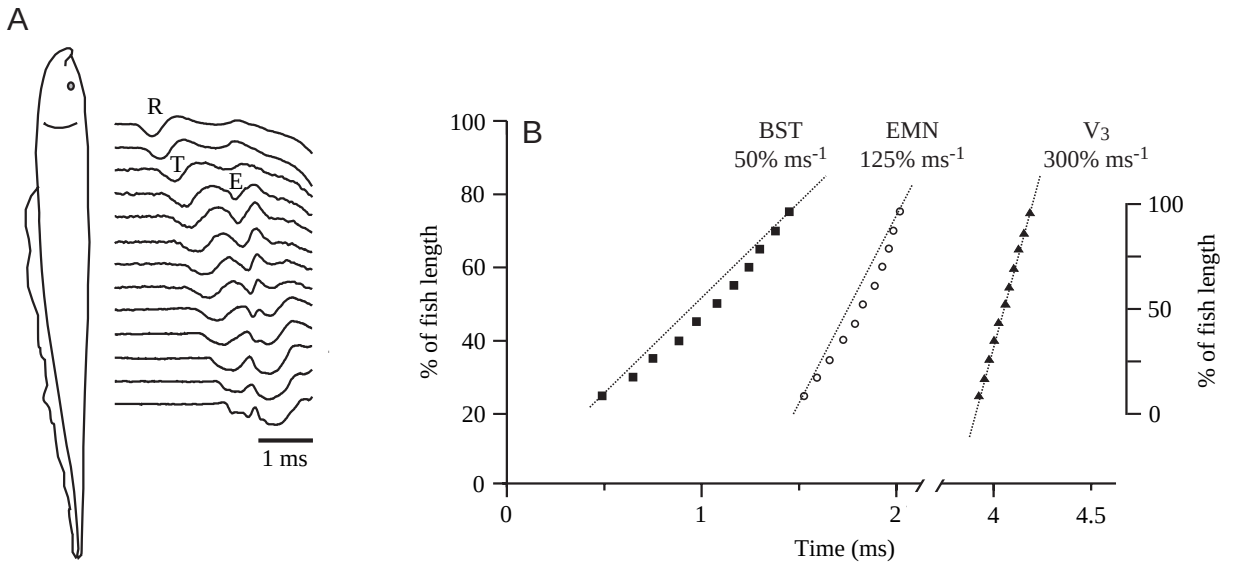

Fig. 10. (A) Surface field potentials recorded using electric organ discharge (EOD)-triggered averaging. Recordings were obtained from the dorsal surface of the fish at consecutive intervals of 5 % of the fish length with a pair of electrodes oriented sagittally and spaced 2 mm apart. The top trace corresponds to the caudal limit of the cranium. R, relay nucleus activation; T, bulbo-spinal tract activation; E, electromotor neurone (EMN) activation. (B) Delays R–T (squares) and R–E (circles) plotted as a function of the recording site along the spinal cord (left abscissa). Delay R–V_3 (triangles), representing the whole time from activation of the relay nucleus to activation of the caudally innervated electrocytes, is plotted as a function of the recording site along the electric organ (EO) (right abscissa). Abscissa and ordinate positions were inverted in order to compare graphically the activation speeds along the fish. Right and left abscissas were constructed taking into account the function relating EMN location and their target EO zone. The slopes of the dotted lines correspond to the mean conduction speeds along the bulbo-spinal tract (BST), the EMN row and the series of caudally innervated electrocytes (V_3) from the origins to ends of their respective domains. Because of the relative expansion of the EMN target domain, when this slope was calculated using the right axis, the electrocyte activation sequence was 2.4 times faster than the EMN activation sequence.

(1990). However, the analysis of timing differences suggests that other synergetic mechanisms should be present also.

Local field potentials also show the activity of the EMNs near the recording site. The delay between the composite bulbo-spinal volley and the EMNs grows smaller from rostral to caudal along the length of the spinal cord. In addition, Albe-Fessard and Martins-Ferreira (1953) and Albe-Fessard (1954) showed *in vitro* that the delay between the descending volley and motor root activation is greater in preparations obtained from rostral segments than in preparations obtained from caudal segments of the spinal cord. These findings led to the conclusion that caudal EMNs are recruited more efficiently than rostral EMNs. One explanation of this phenomenon may be that the temporal dispersion of EMN synaptic input diminishes along the spinal cord, with a consequent enhancement of temporal summation efficacy.

The data of Caputi and Aguilera (1996) indicate that EMN activation follows a rapid sequence along the cord. The EMN field potential occurs sequentially along the cord. The peak of the EMN's potential at the rostral end of the EMN's domain occurs approximately 0.5 ms earlier than the peak of the EMN's potential at the caudal end of the EMN's domain. Considering that this domain is approximately 60 % of fish length, a mean travelling speed of 1.25 L ms^{-1}, where L is fish length, can be calculated for the activation of EMNs along the spinal cord. The peak of V_3 in the abdominal region of the EO occurs 0.3 ms earlier than the peak of V_3 in the caudal region of the EO, yielding a travelling speed of 3.3 L ms^{-1} for the activation of electrocytes along the EO, suggesting that there may be a peripheral mechanism of synchrony. Such a peripheral mechanism is partially related to the relative expansion of the target domain. While the EMN column projecting to the caudal face of electrocytes occupies 60 % of the fish length, the longitudinal domain of caudally innervated electrocytes is the whole EO (occupying 90 % of the fish).

In fish exhibiting a multiphasic EOD waveform, the network must activate sequentially the different sets of homologous electrocyte faces. Data obtained from *G. carapo* suggest that wave sequencing may be based on EMN size and location. Studies using reduced silver impregnation techniques and retrograde labelling methods have revealed two morphological types of EMN: ones with a small, round soma, and others with a large, oval soma. Small, round neurones are 25–40 μm in diameter and bear fine dendrites lacking spines. In contrast, large, oval neurones are 45–60 μm along their major axis and have thick dendritic branches reaching 200 μm in length. The rostral regions of the spinal cord contain exclusively small, round EMNs; in the intermediate portions, large and small neurones co-exist; the caudal region contains only large neurones (Caputi and Trujillo-Cenóz, 1994).

Retrograde labelling experiments revealed that the rostral face of the abdominal electrocytes mediating V_1 is innervated

by a distinct pool of small, round EMNs located within the first seven spinal segments (Caputi and Trujillo-Cenóz, 1994). Since the proportion of slow fibres vanishes at the rostral limit of the domain of the large, oval EMNs (Lorenzo et al., 1990), it is likely that slow fibres and a pool of small, round EMNs constitute a quasi-private path driving V_1. Consistently, when single RN somata were driven by intracellular stimulation, a subset of them provoked head-negative 'unit EOD' responses exclusively in the abdominal region of the EO (Lorenzo et al., 1993). Since segmental nerves innervate the rostral face of abdominal electrocytes, this path is much shorter than the electromotor path serving the caudal face of abdominal electrocytes. Recurrent fibres of the AEN activate the caudal face, adding a significant conduction distance and delay.

Labelling of large, oval EMNs by horseradish peroxidase injections at the AENs and PENs indicate that they project onto the caudal face of abdominal and tail electrocytes (Caputi and Trujillo-Cenóz, 1994). There is no accurate evidence concerning the cell type projecting to the electrocytes in the central portion of the EO. However, indirect evidence suggests that the small round EMNs in this central region might innervate the rostral face of tube 1 electrocytes and thus trigger V_2. First, the domain of doubly innervated electrocytes along the EO is in register with the domain of the small, round EMNs along the spinal cord. Second, submaximal stimulation of electromotor nerves in the intermediate portion of the fish provoked endplate potentials only on the caudal face of doubly innervated electrocytes (Macadar et al., 1989). This difference in threshold indicates that the diameter of fibres projecting to the caudal face is larger than the diameter of fibres projecting to the rostral face. If, as seems likely, fibre and soma diameters correspond, then large neurones would innervate caudal faces and small neurones would innervate rostral faces.

On the basis of these experiments, Caputi and Trujillo-Cenóz (1994) hypothesised that the orderly recruitment of EMNs of different size projecting to different sets of electromotor faces can explain how the sequence V_2–V_3 is organised. This hypothesis would be a new example of Henneman's size principle: large neurones innervating large numbers of electrocytes would be recruited later and with a lower safety factor than small neurones (Hennemann, 1957). Thus, the activation of rostral faces would precede the activation of caudal faces.

Aguilera and Caputi (1994) tested some consequences of this hypothesis. They first activated the bulbo-spinal electromotor tract orthodromically with different stimulation intensities. If small, round EMNs driving rostral faces are more excitable than large, oval EMNs driving caudal faces, then the order of recruitment should depend on the number of afferent fibres stimulated. In confirmation of this hypothesis, threshold intensities evoked only V_2-like, head-negative EO responses. As stimulation intensity was increased, relatively smaller and desynchronised positive V_3-like waves were evoked after the V_2-like response. These V_3-like waves and the following late negative waves (V_4) become progressively more organised as stimulation intensity was increased further, and the natural EOD waveform (V_2–V_3–V_4) was reproduced when the spinal cord was stimulated at 2–2.5 times threshold (Fig. 11A). Strikingly, when the bulbo-spinal electromotor tract was activated antidromically, the resulting EO responses were similar to those for orthodromic activation. This result confirms that the relevant input for the orderly recruitment of the EMN pool is the number of active RN axons (Fig. 11B).

These experiments are compatible with the 'size principle hypothesis' (Hennemann, 1957). However, they do not exclude other peripheral mechanisms that may act synergistically. Such an alternative derives from the findings of Macadar et al. (1989), suggesting that efficacy at the peripheral synapse may also be involved. As observed in Fig. 6B, even when the neural signal reaches the caudal face before it reaches the rostral face, the electrocyte action potential still occurs first at the rostral face.

Our present integrative hypothesis is illustrated in Fig. 12, which refers to the EOD of *G. carapo*. Excitation of the system begins with a single command signal at the relay nucleus. The RN axons convey axon potentials at different velocities along the spinal cord; the shorter the axon, the lower the speed (Fig. 12A). The volley first reaches the small, round EMNs lying in the rostral segments of the cord and projecting to the rostral face of the abdominal electrocytes (Fig. 12B). After 2 ms, most descending fibres are active at the central portion of the cord, projecting onto a mixed-type EMN population (Fig. 12C). At the same time, the postsynaptic potentials occurring at the rostral face of abdominal electrocytes are generating V_1. While V_1 is occurring at rostral levels, the descending volley reaches the caudal segments of the cord. Smaller neurones projecting to the rostral face of central electrocytes are recruited before large neurones projecting to the caudal face of abdominal electrocytes. Approximately 3.5 ms after the command, small EMNs activate electrocyte rostral faces in the central region, generating V_2 (Fig. 12D);

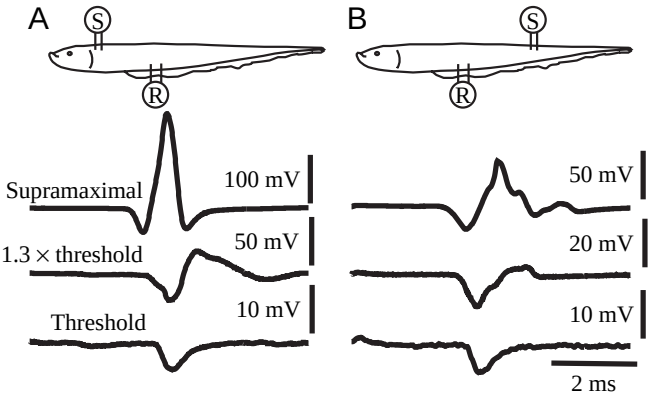

Fig. 11. Electric organ responses evoked by stimulation of the spinal cord. The fish was isolated in air, and the drop in voltage between a pair of electrodes was measured. In both cases, these electrodes (R) were placed at 35 % and 40 % of the fish's length measured from the rostral pole. A pair of stimulation electrodes (S) (sagittally oriented, 2 mm apart) was placed at 15 % (A) (orthodromic) and 70 % (B) (antidromic) of the fish's length measured from the rostral pole.

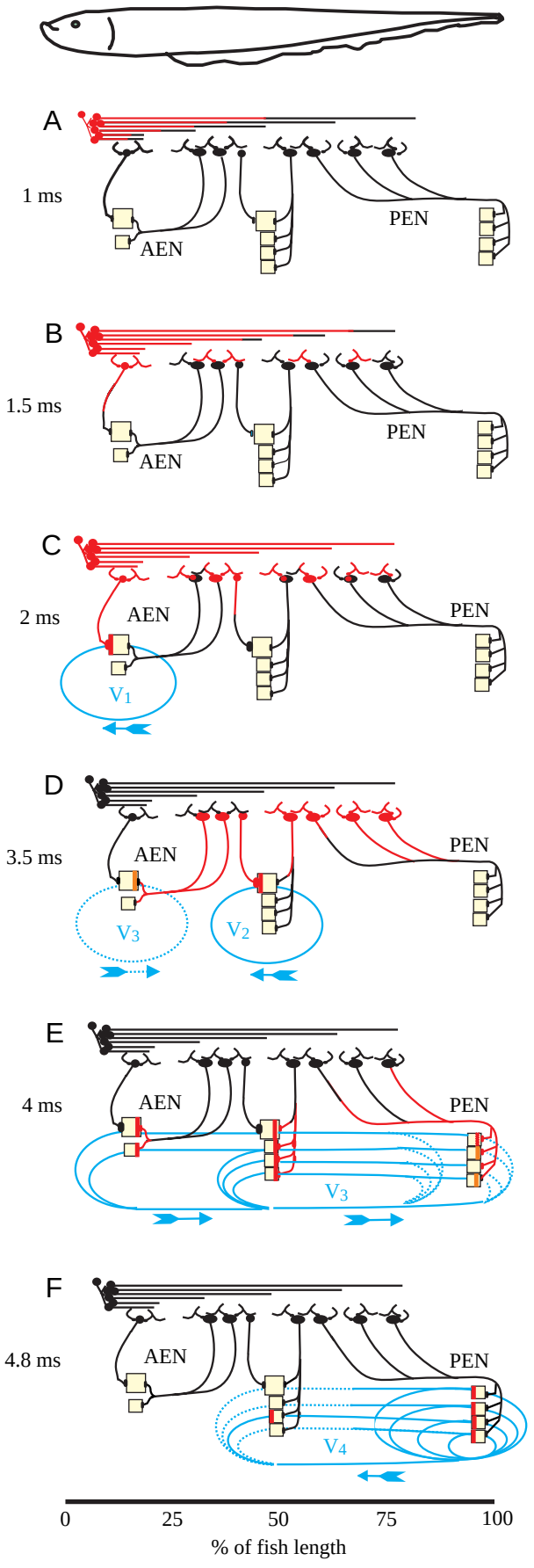

less-excitable large, oval EMNs fire later. This, and possibly the differential efficacy at peripheral synapses, determines that V_3 occurs 0.7 ms later than V_2. Axons of large EMNs projecting to the caudal face of abdominal electrocytes follow a recurrent course through the AEN, adding an extra delay and compensating for some of the differences in spinal conduction times. Thus, activation of the caudal face of abdominal electrocytes occurs after activation of the rostral face in more caudal regions. Large EMNs occupying the most caudal spinal segments project onto the caudal EO through the PEN, eliciting the tail constituent V_3 approximately 4.1 ms after the RN discharge (Fig. 12E). V_4 results when the action potentials generating V_3 propagate to the rostral face of caudally innervated electrocytes. Thus, neural activation of caudal faces elicits the biphasic complex V_3–V_4 (Fig. 12F). However, membrane properties, modulated by endocrine and environmental factors, determine the shape of V_4. The currents locally generated by electrocyte subsets flow within the internal tissues and the surrounding medium so that the fish body behaves as a distributed electric source.

Discussion

Understanding how the central nervous system transforms a single impulse into a complex and stereotyped electromotor pattern is relevant not only for electric fish physiology but also for gaining knowledge about general mechanisms of motor coordination.

It is important to distinguish the action of the electromotor system from the EOD-associated field. The first reflects the ability of the fish to generate external currents, while the second is the actual pattern of potential and emitted currents when the fish's equivalent source is loaded by a particular surrounding impedance. The first is the necessary consequence of the EO activation; the second is contingent upon the medium. Therefore, the output of the electromotor system should be defined as the fish's equivalent source and should be described by its parameters.

In pulse gymnotids, the output of the electromotor system is a complex spatio-temporal pattern of an EMF and an inhomogeneous internal resistance. In contrast, the input to the electromotor system is a localised impulse-like pacemaker discharge. Therefore, the nervous system must combine temporal and spatial processing of such simple input to achieve a complex electrogenic output.

Both the duration and temporal order of output wave components are determined with singular precision. This is

Fig. 12. Activation of the electromotor system at different times after the pacemaker discharge. The active structures are shown schematically in red for each time (A–F). The electrocyte synaptic currents and action currents that give rise to the electric organ discharge (EOD) wave components are represented in blue. A detailed explanation of each phase can be found in the text. AEN, anterior electromotor nerve; PEN, posterior electromotor nerve; V_1–V_4, phases of the EOD.

achieved by activation of different effector elements distributed along the EO according to a species-specific pattern. This process appears to be supported by the synergistic action of neural delay lines that are implemented in a variety of forms. In the particular case of *G. carapo*, these include (1) different conduction velocities along the spinal cord, (2) different conduction distances in the periphery and (3) an appropriate distribution of coupling delays (included within this term are the conduction time through fine terminals, synaptic delay and synaptic efficacy). In this system, consistency and effectiveness are redundantly ensured by multiple mechanisms, and as yet undiscovered strategies for time processing cannot be definitively discarded.

In addition, both convergent and divergent processes strongly contribute to the precision and stability of the system. This overlapping strategy is not exclusive to the electromotor system. In the primate pyramidal system, single cortical neurones facilitate functional subsets of muscles in the forelimb. Clusters of neurones facilitate the same muscle, and each muscle is represented many times over in the cortex (Lemon, 1988).

Comparative studies indicate that similar processes occur in all species of 'pulse' gymnotids. However, species-specific EOD waveforms depend on particular EO innervation patterns and on the particular membrane properties of electrocytes. The hormonal effects described for *B. pinnicaudatus* and the thermal effects observed in *G. carapo* and *B. pinnicaudatus* should be noted as evidence of the plastic properties of electrocytes (Caputi et al., 1998). While the nervous system appears to be designed to perform a fixed transformation rule for each species, peripheral effector and post-effector structures appear to be the elements that support individual profiles and adaptive behaviours.

This article summarises the results of a multidisciplinary research project on the electrogenic system. Omar Trujillo-Cenóz and Omar Macadar pioneered the enterprise in 1983 and have contributed with useful suggestions and comments to this manuscript. Pedro Aguilera, Jose Luis Ardanaz, Cristina Bertolotto, Ruben Budelli, Virginia Comas, Gustavo Dittrich, Juan Antonio Echagüe, Juan Vicente Echagüe, Daniel Lorenzo, Felipe Sierra, Ana Celia Silva and Julio Cesar Velluti also participated in different aspects of this research. The author thanks Drs Curtis Bell, Kirsty Grant, Len Maler, Ray Turner and Walter Meltzer for the critical reading and comments on the manuscript.

References

Aguilera, P. and Caputi, A. (1994). Mecanismos espinales de la organización de la forma de onda en *Gymnotus carapo*. *Resumenes del XVIII Congreso Latiniamericano de Ciencias Fisiologicas*. 221pp. Montevideo, Uruguay.

Aguilera, P. and Caputi, A. (1995). Organización espinal de la descarga del organo electrico (DOE) en *Gymnotus carapo*: Un modelo simple basado en datos experimentales. *Resumenes de las VII Jornadas Cientificas de la Sociedad Uruguaya de Biociencias*. 97pp. Piriapolis. Uruguay.

Albe-Fessard, D. (1954). Novelle etude des latences spinales dans le dispositif de commande des organs electriques chez *Electrophorus electricus*. *Anais Acad. Brasil. Cienc*. **26**, 187–192.

Albe-Fessard, D. and Buser, P. (1950). Etude de l'interaction par chamo électrique entre deux fragments d'organe de torpille (*Torpedo marmorata). J. Physiol., Paris* **42**, 528–529.

Albe-Fessard, D. and Martins-Ferreira, H. (1953). Role de la commande nerveuse dans la synchronization du fonctionnement des éléments de l'organ électrique du Gymnote *Electrophorus electricus* L. *J. Physiol., Paris* **45**, 533–546.

Ardanaz, J. L. (1998). Efectos de la temperatura sobre la forma de onda de *G. carapo*. MSc thesis, PEDECIBA, Montevideo, Uruguay.

Baillet-Derbin, C. (1988). Motoneuron organization in the spinal cord of three teleost fishes, *Gymnotus carapo* (Gymnotidae), *Gnathonemus petersii* (Mormyridae) and *Salmo trutta* (Salmonidae). *Biol. Struct. Morphogen.* **1**, 160–170.

Bass, A. H. (1986). Electric organs revisited: evolution of a vertebrate communication and orientation organ. In *Electroreception* (ed. T. H. Bullock and W. Heiligenberg), pp. 13–70. New York: Wiley.

Bass, A. H. and Hopkins, C. D. (1983). Hormonal control of sexual differentiation: changes in electric organ discharge waveform. *Science* **220**, 971–974.

Bastian, J. (1986). Electrolocation: behavior, anatomy and physiology. In *Electroreception* (ed. T. H. Bullock and W. Heiligenberg,), pp. 577–612. New York: Wiley.

Bell, C. C. (1989). Sensory coding and corollary discharge effects in mormyrid electric fish. *J. Exp. Biol.* **146**, 229–253.

Bell, C. C., Bradbury, J. and Russell, C. J. (1976). The electric organ of a mormyrid as a current and voltage source. *J. Comp. Physiol.* A **110**, 65–88.

Bennett, M. V. L. (1971). Electric organs. In *Fish Physiology*, vol. V (ed. W. S. Hoar and D. J. Randall), pp. 347–491. London: Academic Press.

Bennett, M. V. L., Gimenez, M., Nakajima, Y. and Pappas, G. D. (1964). Spinal and medullary nuclei controlling the electric organ in the eel, *Electrophorus electricus. Biol. Bull.* **127**, 362.

Bennett, M. V. L. and Grundfest, H. (1959). Electrophysiology of electric organ in *Gymnotus carapo*. *J. Gen. Physiol.* **42**, 1067–1104.

Bennett, M. V. L., Sandri, C. and Akert, K. (1978). Neuronal gap junctions and morphologically mixed synapses in the spinal cord of a teleost, *Sternarchus albifrons* (Gymnotoidei). *Brain Res.* **143**, 43–60.

Bennett, M. V. L., Pappas, G. D., Aljure, E. and Nakajima, Y. (1967). Physiology and ultrastructure of electrotonic junctions. II. Spinal and medullary electromotor nuclei in mormyrid fish. *J. Neurophysiol.* **30**, 180–208.

Black-Cleworth, P. (1970). The role of electrical discharges in the non-reproductive social behaviour of *Gymnotus carapo* (Gymnotidae, Pisces). *Anim. Behav. Monogr.* **3**, 1–77.

Bullock, T. H., Fernandez–Souza, N., Graf, W., Heiligenberg, W., Langner, G., Mayer, D. L., Pimmentel-Souza, F., Scheich, H. and Viancour, T. A. (1979). Aspectos do uso da descarga do urgano electrico e electrorecepçao nos gymnotoidei e outros peices amazonicos. *Acta Amazonica* **9**, 549–572.

Bullock, T. H. and Heiligenberg, W. (1986). (eds) *Electroreception*. New York: Wiley. 722pp.

Camhi, J. M. (1984). *Neuroethology. Nerve Cells and the Natural Behavior of Animals*. Sunderland, MA: Sinauer Associates. 416pp.

Caputi, A. and Aguilera, P. (1996). A field potential analysis of the electromotor system in *Gymnotus carapo*. *J. Comp. Physiol.* A **179**, 827–835.

Caputi, A. and Budelli, R. (1995). The electric image un weakly electric fish. I. A data-based model of waveform generation in *Gymnotus carapo*. *J. Comput. Neurosci.* **2**, 131–147

Caputi, A., Macadar, O. and Trujillo-Cenóz, O. (1989). Waveform generation in *Gymnotus carapo*. III. Analysis of the fish body as an electric source. *J. Comp. Physiol.* A **165**, 361–370.

Caputi, A., Macadar, O. and Trujillo-Cenóz, O. (1994). Waveform generation in *Rhamphichthys rostratus* (L.) (Teleostei, Gymnotiformes). The electric organ and its spatiotemporal activation pattern. *J. Comp. Physiol.* A **174**, 633–642.

Caputi, A., Silva, A. and Macadar, O. (1993). Electric organ activation in *Gymnotus carapo*: spinal and peripheral mechanisms. *J. Comp. Physiol.* A **173**, 227–232.

Caputi, A., Silva, A. and Macadar, O. (1998). The effect of environmental variables on waveform generation in *Brachyhypopomus pinnicaudatus*. *Brain Behav. Evol.* **52**, 148–158.

Caputi, A. and Trujillo-Cenóz, O. (1994). The spinal cord of *Gymnotus carapo*: the electromotorneurons and their projection pattern. *Brain Behav. Evol.* **44**, 166–174.

Coates, C. W., Altamirano, M. and Grundfest, H. (1954). Activity in electrogenic organs of knifefishes. *Science* **120**, 845–846.

Coates, C. W., Cox, R. T. and Granath, L. P. (1937). The electric discharge of the electric eel, *Electrophorus electricus* (Linneaus). *Zoologica* **22**, 1–34.

Coates, C. W., Cox, R. T., Rosemblith, W. A. and Brown, M. B. (1940). Propagation of the electric impulse along the organs of the electric eel, *Electrophorus electricus* (Linnaeus). *Zoologica* **25**, 249–256.

Couceiro, A. and De Almeida, D. F. (1961). The electrogenic tissue of some gymnotidae. In *Bioelectrogenesis* (ed. C. Chagas and A. Paes de Carvalho), pp. 3–13. Amsterdam: Elsevier.

Cox, R. T. and Coates, C. W. (1938). Electrical characteristics of the electric tissue of the electric eel *Electrophorus electricus* (Linnaeus). *Zoologica* **23**, 203–212.

Donaldson, P. E. K. (1958). *Electronic Apparatus for Biological Research*. London: Butterworth.

Ellis, D. B. and Szabo, T. (1980). Identification of different cell types in the command (pacemaker) nucleus of several gymnotiform species by retrograde transport of horseradish peroxidase *Neurosci.* **5**, 1917–1929.

Ferrari, M. B. and Zakon, H. H. (1993). Conductances contributing to the action potential of *Sternopygus* electrocytes. *J. Comp. Physiol.* A **173**, 281–292.

Fessard, A. (1958). Les organes électriques. In *Traité de Zoologie*, vol. 13, *Agnathes et Poissons: Anatomie, Éthologie, Systématique* (ed. P. P. Grassé), pp. 1143–1238. Paris: Masson.

Finger, T. E., Bell, C. C. and Carr, C. E. (1986). Comparisons among electroreceptive teleosts: why are electrosensory systems so similar? In *Electroreception* (ed. T. H. Bullock and W. Heiligenberg), pp. 465–481. New York: Wiley.

Franchina, C. R. (1993). The waveform of the weakly electric fish *Hypopomus pinnicaudatus* changes daily in the male. In *Contributions of Electrosensory Systems to Neurobiology and Neuroethology. Proceedings of a Conference in Honor of the Scientific Career of Thomas Szabo* (ed. C. C. Bell, C. D. Hopkins and K. Grant). *J. Comp. Physiol.* A **173**, 742.

Hagedorn, M. and Carr, C. (1985). Single electrocytes produce a sexually dimorphic signal in South American electric fish, *Hypopomus occidentalis* (Gymnotiformes, Hypopomidae). *J. Comp. Physiol.* A **156**, 511–523.

Harder, W., Schief, A. and Uhlemann, H. (1964). Zur function des elektrische organs von *Gnathonemus petersii* (Gthr. 1862) (Mormyriformes, Teleostei). *Z. Vergl. Physiol*. **48**, 302–331.

Helmholtz, H. (1853). Ueber einige Gesetze der Verteilung elektrischer Ströme in köperlichen Leitern mit Anwendung auf die thierisch-elektrischen Versuche. *Pogg. Ann. Physik Chemie.* **89**, 211–233.

Hennemann, E. (1957). Relation between size of neurons and their susceptibility to discharge. *Science* **126**, 1345–1346.

Hopkins, C. D. (1981). The neuroethology of electric communication. *Trends Neurosci.* **4**, 4–6.

Hopkins, C. D. (1995). Convergent design for electrogenesis and electroreception. *Curr. Opin. Neurobiol.* **5**, 769–777.

Hopkins, C. D., Comfort, N. C., Bastian, J. and Bass, A. H. (1990). Functional analysis of sexual dimorphism in an electric fish, *Hypopomus pinnicaudatus*, order Gymnotiformes. *Brain Behav. Evol.* **35**, 350–367.

Hoshimiya, N., Shogen, K., Matsuo, T. and Chichibu, S. (1980). The *Apteronotus* EOD field: Waveform and EOD field simulation. *J. Comp. Physiol.* A **135**, 283–290.

Keynes, R. D., Bennett, M. V. L. and Grundfest, H. (1961). Studies on the morphology and electrophysiology of electric organs. II. Electrophysiology of the electric organ of *Malapterurus electricus*. In *Bioelectrogenesis* (ed. C. Chagas and A. Paes de Carvalho), pp. 102–112. Amsterdam: Elsevier.

Kramer, B. (1990). *Electrocommunication in Teleost Fishes: Behavior and Experiments*. New York: Springer. 240pp.

Landsman, R. E. and Moller, P. (1988). Testosterone changes the electric organ discharge and external morphology of the mormyrid fish, *Gnathonemus petersii* (Mormyriformes). *Experientia* **44**, 900–903.

Lemon, R. (1988). The output map of the motor cortex. *Trends Neurosci*. **11**, 501–506.

Lissmann, H. W. (1951). Continuous electrical signals from the tail of a fish, *Gymnarchus niloticus* Cuv. *Nature* **167**, 201–202.

Lopez da Silva, F. and van Rotterdam, A. (1982). Biophysical aspects of EEG and MEG generation. In *Electroencephalogaphy* (ed. E. Niedermeyer and F. Lopez da Silva), pp. 15–26. Baltimore, MA: Urban & Schwarzenberg.

Lorenzo, D., Sierra, F., Silva, A. and Macadar, O. (1990). Spinal mechanisms of electric organ discharge synchronization in *Gymnotus carapo*. *J. Comp. Physiol.* A **167**, 447–452.

Lorenzo, D., Sierra, F., Silva, A. and Macadar, O. (1993). Spatial distribution of the medullary command signal within the electric organ of *Gymnotus carapo*. *J. Comp. Physiol.* A **173**, 233–238.

Lorenzo, D., Velluti, J. C. and Macadar, O. (1988). Electrophysiological properties of abdominal electrocytes in the weakly electric fish *Gymnotus carapo*. *J. Comp. Physiol.* **162**, 141–144.

Macadar, O. (1993). Motor control of waveform generation in *Gymnotus carapo. J. Comp. Physiol* A **173**, 728–729.

Macadar, O., Lorenzo, D. and Velluti, J. C. (1989). Waveform generation of the electric organ discharge in *Gymnotus carapo.* II. Electrophysiological properties of single electrocytes. *J. Comp. Physiol.* A **165**, 353–360.

Mezler, R. M., Pappas, G. D. and Bennett, M. V. L. (1974). Morphology of the electromotor system in the spinal cord of the electric eel *Electrophorus electricus*. *J. Neurocytol.* **3**, 251–261.

Mills, A. and Zakon, H. H. (1987). Coordination of EOD frequency and pulse duration in weakly electric wave fish: the influence of androgens. *J. Comp. Physiol.* A **161**, 417–430.

Moller, P. (1995). *Electric Fishes, History and Behaviour*. London: Chapman & Hall, 181pp.

Rasnow, B. (1996). The effects of simple objects on the electric field of *Apteronotus. J. Comp. Physiol.* A **178**, 397–411.

Rasnow, B., Assad, C. and Bower, J. M. (1993). Phase and amplitude maps of the electric organ discharge of the weakly electric fish *Apteronotus leptorhynchus. J. Comp. Physiol.* A **172**, 481–491.

Rasnow, B. and Bower, J. M. (1996). The electric organ discharges of the gymnotiform fishes. I. *Apteronotus leptorhynchus. J. Comp. Physiol.* A **178**, 383–396.

Schaffer, E. L. (1917). On the electric organ of *Gymnotus carapus. Science* **45**, 67–69.

Silva, A., Caputi, A., Galeano, M., Errandonea, P., Eiris, G. and Budelli, R. (1996). Natural and evoked sexual dimorphism in the weakly electric fish *Hypopomus* sp. *Neurosci Abstr* **179**, 7.

Szabo, T. (1960). Quelques observations sur l'innervation de l'organ electrique de *Gymnotus carapo. Arch. Anat. Microsc. Morphol. Exp*. **49**, 89–92.

Szabo, T. (1961a). Les organes électriques de *Gymnotus carapo*. *Proc. K. Ned. Akad. Wet. Ser.* **64**, 584–586.

Toerring, M.-J. and Serrier, J. (1978). Influence of water temperature on the electric organ discharge (EOD) of the weakly electric fish *Marcusenius cyprinoides* (Mormyridae). *J. Exp. Biol.* **74**, 133–150.

Trujillo-Cenóz, O. and Echagüe, J. A. (1989). Waveform generation of the electric organ discharge in *Gymnotus carapo.* I. Morphology and innervation of the electric organ. *J. Comp. Physiol.* A **165**, 343–351.

Trujillo-Cenóz, O., Echagüe, J. A., Bertolotto, C. and Lorenzo, D. (1986). Some aspects of the structural organization of the spinal cord of *Gymnotus carapo* (Teleostei, Gymnotiformes). I. The electromotor neurons. *J. Ultrastruct. Mol. Struct. Res.* **97**, 130–143.

Trujillo-Cenóz, O., Echagüe, J.A. and Macadar, O. (1984). Innervation pattern and electric organ discharge waveform in *Gymnotus carapo*. *J. Neurobiol*. **15**, 273–281.

Trujillo-Cenóz, O., Lorenzo, D. and Caputi, A. (1990). Waveform generation of the electric organ discharge in *Gymnotus carapo*. I. Anatomical aspects. In *Fundamental Neurobiology* (ed. E. Garcia Austt, O. Macadar, O. Trujillo-Cenoz and R. Velluti), pp. 197–205. Montevideo, Uruguay: Departamento de Publicaciones. Universidad de la Republica.

Watson, D. and Bastian, J. (1979). Frequency response characteristics of electroreceptors in the weakly electric fish *Gymnotus carapo*. *J. Comp. Physiol.* A **134**, 191–202.

Zakon, H. H. (1993). Weakly electric fish as model systems for studying long-term steroid action on neural circuits. *Brain Behav. Evol.* **42**, 242–251.

Zakon, H. H., Mills, A. C. and Ferrari, M. B. (1991a). Androgen-dependent modulation of the electrosensory and electromotor systems of a weakly electric fish. *Sem. Neurosci.* **3**, 449–457.

Zakon, H. H., Thomas, P. and Yan, H. Y. (1991b). Electric organ discharge frequency and plasma sex steroid levels during gonadal recrudescence in a natural population of *Sternopygus macrurus*. *J. Comp. Physiol.* A **169**, 493–499.